

2014

NLO Hierarchy of Wilson Lines Evolution

I. Balitsky
Old Dominion University

Follow this and additional works at: https://digitalcommons.odu.edu/physics_fac_pubs

 Part of the [Physics Commons](#)

Repository Citation

Balitsky, I., "NLO Hierarchy of Wilson Lines Evolution" (2014). *Physics Faculty Publications*. 71.
https://digitalcommons.odu.edu/physics_fac_pubs/71

Original Publication Citation

Balitsky, I. (2015). NLO hierarchy of Wilson lines evolution. *International Journal of Modern Physics: Conference Series*, 37, 1560056.
doi:10.1142/s2010194515600563

NLO Hierarchy of Wilson Lines Evolution

I. Balitsky

*Department of Physics, Old Dominion University,
Norfolk VA 23529, USA*

*Theory Center, Jefferson Lab, 12000 Jefferson Ave,
Newport News, VA 23606, USA
balitsky@jlab.org*

Published 25 February 2015

The high-energy behavior of QCD amplitudes can be described in terms of the rapidity evolution of Wilson lines. I present the hierarchy of evolution equations for Wilson lines in the next-to-leading order.

Keywords: Rapidity evolution; high energy; Wilson lines.

PACS numbers: 12.38.Bx, 12.38.Cy

1. Introduction

A well-known general feature of high-energy scattering is that a fast particle moves along its straight-line classical trajectory and the only quantum effect is the eikonal phase factor acquired along this propagation path. In QCD, for the fast quark or gluon scattering off some target, this eikonal phase factor is a Wilson line - the infinite gauge link ordered along the straight line collinear to particle's velocity. This observation serves as a starting point in the analysis of high-energy amplitudes by operator expansion in Wilson lines developed in Ref. [1].

This approach is based on factorization in rapidity² and the cornerstone of the method is the evolution of Wilson-line operators with respect to their rapidity. In a few sentences, the basic outline of this approach is the following (for reviews, see Refs. [3, 4]). First, we introduce a "rapidity divide" η between rapidity of the projectile Y_P and rapidity of the target Y_T and separate all Feynman loop integrals over longitudinal momentum (\equiv rapidity) in two parts: in coefficient functions (called impact factors) with $Y > \eta$ and matrix elements of Wilson-line operators with $Y < \eta$. As we mentioned above, interaction of fast particles with the slow ones can

This is an Open Access article published by World Scientific Publishing Company. It is distributed under the terms of the Creative Commons Attribution 3.0 (CC-BY) License. Further distribution of this work is permitted, provided the original work is properly cited.

be described in the eikonal approximation so the relevant operators are Wilson lines. Second, we find the evolution equations for these Wilson-line operators with respect to our rapidity factorization scale η . Third, we solve these equations (analytically or numerically) and evolve the Wilson-line operators down to the energies of few GeV at which step we need to convolute the results with the initial conditions for the rapidity evolution. If the target is can be described by perturbative QCD (like virtual photon or heavy-quark meson) these initial conditions can be calculated in pQCD. If the target is a proton or nucleus, the initial conditions are usually taken in the form of Mueller-Glauber model.

The most well-studied part is the evolution of the “color dipole” (the trace of two Wilson lines) which has a great number of phenomenological applications. The evolution of color dipoles is known both in the leading order (the BK equation [1, 5]) and in the next-to-leading order (NLO) [6, 7] and the solutions of the BK with running α_s [8, 9] are widely used for pA and heavy-ion experiments at LHC and RHIC. However, recently it was realized that many interesting processes are described by the evolution of more complicated operators such as “color quadrupoles” (trace of four Wilson lines) [10]. To describe such evolution the NLO BK must be generalized to the full hierarchy of Wilson-lines evolution. In this publication I present the final results for the kernels and the example of the NLO kernel for the most simple non-dipole operator - the “color tripole” relevant for baryon scattering.

2. High-Energy OPE and Rapidity Factorization

Consider an arbitrary Feynman diagram for scattering of two particles with momenta $p_A = p_1 + \frac{p_A^2}{s} p_2$ and $p_B = p_2 + \frac{p_B^2}{s} p_1$ ($p_1^2 = p_2^2 = 0$). Following standard high-energy OPE logic we introduce the rapidity divide η which separates the “fast” gluons from the “slow” ones. As a first step, we integrate over gluons with rapidities $Y > \eta$ and leave the integration over $Y < \eta$ to be performed afterwards. It is convenient to use the background field formalism: we integrate over gluons with $\alpha > \sigma = e^\eta$ and leave gluons with $\alpha < \sigma$ as a background field, to be integrated over later. Since the rapidities of the background gluons are very different from the rapidities of gluons in our Feynman diagrams, the background field can be taken in the form of a shock wave due to the Lorentz contraction. The integrals over gluons with rapidities $Y > \eta$ give the so-called impact factors -coefficients in front of Wilson-line operators with the upper rapidity cutoff η for emitted gluons. The Wilson lines are defined as

$$\begin{aligned}
 U_x^\eta &= P \exp \left[ig \int_{-\infty}^{\infty} du p_1^\mu A_\mu^\sigma(ux_1 + x_\perp) \right], \\
 A_\mu^\eta(x) &= \int d^4k \theta(e^\eta - |\alpha_k|) e^{ik \cdot x} A_\mu(k)
 \end{aligned}
 \tag{1}$$

where α is Sudakov variable ($p = \alpha p_1 + \beta p_2 + p_\perp$).

The result for the amplitude can be written as

$$A(p_A, p_B) = \sum I_i(p_A, p_B, z_1, \dots, z_n; \eta) \langle p_B | U^\eta(z_1) \dots U^{\dagger\eta}(z_n) | p_B \rangle \quad (2)$$

where the color indices of Wilson lines are convoluted in a colorless way (and connected by gauge links at infinity). As in usual OPE, the coefficient functions (“impact factors” I_i) and matrix elements depend on the “rapidity divide” η but this dependence is cancelled in the sum (2). It is convenient to define the impact factors in an energy-independent way (see e.g. Ref. [11]) so all the energy dependence is shifted to the evolution of Wilson lines in the r.h.s. of Eq. (2) with respect to η .

To find the evolution equations of these Wilson line operators with respect to rapidity cutoff η we again factorize in rapidity. We consider the matrix element of the set of Wilson lines between (arbitrary) target states and integrate over the gluons with rapidity $\eta_1 > \eta > \eta_2 = \eta_1 - \Delta\eta$ leaving the gluons with $\eta < \eta_2$ as a background field (to be integrated over later). In the frame of gluons with $\eta \sim \eta_1$ the fields with $\eta < \eta_2$ shrink to a pancake and we obtain four diagrams of the type shown in Fig. 1. The result of the evolution of Wilson lines can be presented as infinite hierarchy of evolution equations for n-Wilson-line operators. This hierarchy of equations can be constructed from finite number of “blocks” with this number equal to the order of perturbation theory.

It should be mentioned that an alternative approach to high-energy scattering in the dense QCD regime is to write the rapidity evolution of the wavefunction of the target which is governed by the JIMWLK equation.¹² The JIMWLK Hamiltonian summarizes the hierarchy of evolution equations for Wilson-line operators. As it was shown recently in Ref. [13], the hierarchy of equations presented in the next Section can be represented as the NLO correction to JIMWLK Hamiltonian.

3. LO Hierarchy

In the leading order the hierarchy can be built from self-interaction (evolution of one Wilson line) and “pairwise interaction”.

The typical diagrams are shown in Fig. 1 and the equations have the form¹

$$\frac{d}{d\eta} \begin{Bmatrix} (U_1)_{ij} \\ (U_1^\dagger)_{ij} \end{Bmatrix} = \frac{\alpha_s}{\pi^2} \int \frac{d^2 z_4}{z_{14}^2} (U_4^{ab} - U_1^{ab}) \begin{Bmatrix} (t^a U_1 t^b)_{ij} \\ (t^b U_1^\dagger t^a)_{ij} \end{Bmatrix} \quad (3)$$

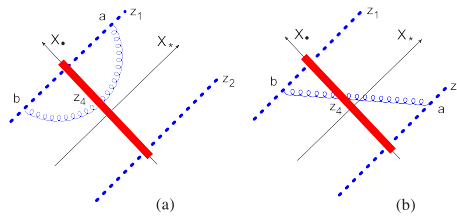


Fig. 1. LO diagrams.

for the self-interaction diagrams of Fig. 1a type and

$$\frac{d}{d\eta} \left\{ \begin{array}{l} (U_1)_{ij}(U_2)_{kl} \\ (U_1)_{ij}(U_2^\dagger)_{kl} \\ (U_1^\dagger)_{ij}(U_2^\dagger)_{kl} \end{array} \right\} = \frac{\alpha_s}{2\pi^2} \int d^2 z_4 [2U_4 - U_1 - U_2]^{ab} \frac{(z_{14}, z_{24})}{z_{14}^2 z_{24}^2} \times \left\{ \begin{array}{l} (t^a U_1)_{ij}(U_2 t^b)_{kl} + (U_1 t^b)_{ij}(t^a U_2)_{kl} \\ -(t^a U_1)_{ij}(t^b U_2^\dagger)_{kl} - (U_1 t^b)_{ij}(U_2^\dagger t^a)_{kl} \\ (U_1^\dagger t^a)_{ij}(t^b U_2^\dagger)_{kl} + (t^b U_1^\dagger)_{ij}(U_2^\dagger t^a)_{kl} \end{array} \right\} \quad (4)$$

for the “pairwise” diagram shown in Fig. 1b. Hereafter we use the notation $U_i \equiv U_{z_i}$ and the integration variable is called z_4 for uniformity of notations in all Sections). All vectors z_i are two-dimensional and (z_i, z_j) is a scalar product.

The evolution equations in this form are correct both in the fundamental representation of Wilson lines where $t^a = \lambda^a/2$ and in the adjoint representation where $(t^a)_{bc} = -if^{abc}$. In the adjoint representation U and U^\dagger are effectively the same matrices ($U_{ab}^\dagger = U_{ba}$) so the three evolution equations (4) are obtained from each other by corresponding transpositions. (One should remember that $(t^a)_{bc} = -(t^a)_{cb}$ in the adjoint representation). Since the color structure of the diagrams in the fundamental representation is fixed one can get the kernels by comparison with adjoint representation. Effectively, since our results will be always presented in the form universal for adjoint and fundamental representations the NLO results for the evolution of $U \otimes U^\dagger$ and $U^\dagger \otimes U^\dagger$ can be obtained by transposition.

4. NLO Hierarchy

In the next-to-leading order (NLO) the hierarchy can be constructed from self-interactions, pairwise interactions, and triple interactions. The typical diagrams are shown in Fig. 2 ab, Fig. 2 cd, and Fig. 2 ef, respectively.

4.1. Self-interaction

The most simple part is the one-particle interaction (“gluon reggeization” term). The typical diagrams are shown in Fig. 2 a,b and the result has the form

$$\begin{aligned} \frac{d}{d\eta} (U_1)_{ij} &= \frac{\alpha_s^2}{8\pi^4} \int \frac{d^2 z_4 d^2 z_5}{z_{45}^2} \left\{ U_4^{dd'} (U_5^{ee'} - U_4^{ee'}) \left(\left[2I_1 - \frac{4}{z_{45}^2} \right] f^{ade} f^{bd'e'} (t^a U_1 t^b)_{ij} \right. \right. \\ &+ \left. \left. \frac{(z_{14}, z_{15})}{z_{14}^2 z_{15}^2} \ln \frac{z_{14}^2}{z_{15}^2} \times [i f^{ad'e'} (\{t^d, t^e\} U_1 t^a)_{ij} - i f^{ade} (t^a U_1 \{t^d, t^e\})_{ij}] \right) \right\} \\ &+ 4(t^a U_1 t^b)_{ij} n_f I_{f1} \text{tr} \{ t^a U_4 t^b (U_5^\dagger - U_4^\dagger) \} + \int \frac{d^2 z_4}{z_{14}^2} \frac{\alpha_s^2 N_c}{4\pi^3} \\ &\times (U_4^{ab} - U_1^{ab}) (t^a U_1 t^b)_{ij} \left\{ \frac{11}{3} \ln \frac{z_{14}^2 \mu^2}{4} + 2C + \frac{67}{9} - \frac{\pi^2}{3} - \frac{n_f}{N_c} \right. \\ &\times \left. \left[\frac{2}{3} \ln z_{14}^2 \mu^2 + \frac{10}{9} \right] \right\}, \quad (5) \end{aligned}$$

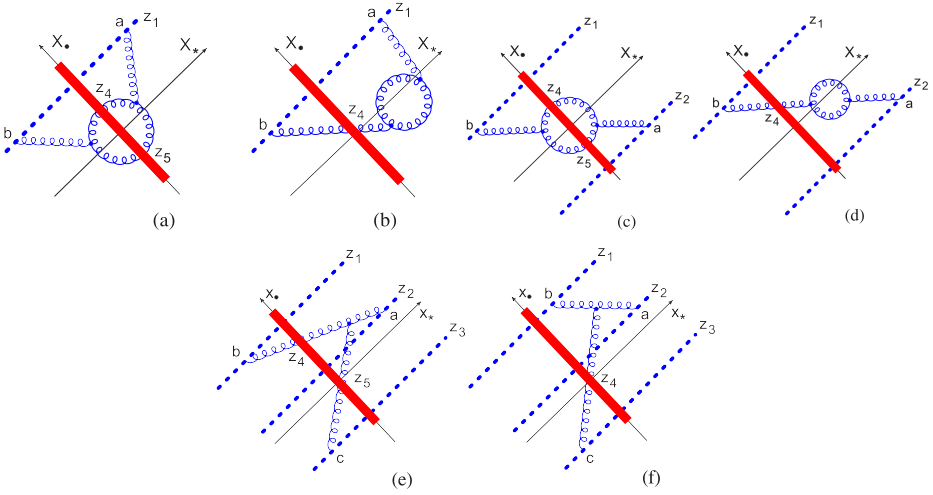


Fig. 2. Typical NLO diagrams.

where n_f is the number of active quark flavors and μ is the normalization point. (The quark diagrams are similar to those in Fig. 2 a-d with the gluon loop replaced by the quark one). Hereafter we use the notations

$$I_1 \equiv I(z_1, z_4, z_5) = \frac{\ln z_{14}^2/z_{15}^2}{z_{14}^2 - z_{15}^2} \left[\frac{z_{14}^2 + z_{15}^2}{z_{45}^2} - \frac{(z_{14}, z_{15})}{z_{14}^2} - \frac{(z_{14}, z_{15})}{z_{15}^2} - 2 \right], \quad (6)$$

$I_2 \equiv I(z_2, z_4, z_5)$, and

$$I_{f1} \equiv I_f(z_1, z_4, z_5) = \frac{2}{z_{45}^2} - \frac{2(z_{14}, z_{15})}{z_{45}^2(z_{14}^2 - z_{15}^2)} \ln \frac{z_{14}^2}{z_{15}^2}. \quad (7)$$

(The integration variables are called z_4 and z_5 for uniformity of notations in all Sections).

The result in this form is correct both in fundamental and adjoint representations. (For quark contribution proportional to n_f one should replace t^a by adjoint representation matrices only in $t^a U_1 t^b$ and leave the fundamental t^a and t^b in the quark loop). As we discussed in previous Section, this means that the results for the evolution of U^\dagger can be obtained by transposition. We have checked the ‘‘transposing rule’’ by explicit calculation.

4.2. Pairwise interaction

The typical diagrams for pairwise interaction are shown in Fig. 2 c,d (and the full set is given by Fig. 6 in Ref. [6]). In this letter we present the final result, the details would be published elsewhere. The evolution equation for $U \otimes U$ has the form

$$\frac{d}{d\eta}(U_1)_{ij}(U_2)_{kl} = \frac{\alpha_s^2}{8\pi^4} \int d^2 z_4 d^2 z_5 (\mathcal{A}_1 + \mathcal{A}_2 + \mathcal{A}_3) + \frac{\alpha_s^2}{8\pi^3} \int d^2 z_4 (\mathcal{B}_1 + N_c \mathcal{B}_2) \quad (8)$$

where the kernels $\mathcal{A}_i(z_1, z_2, z_4, z_5)$ corresponds to diagrams of Fig.2 a,c type and $\mathcal{B}_i(z_1, z_2, z_4)$ to Fig.2 b,d type. The explicit expressions are

$$\begin{aligned} \mathcal{A}_1 &= [(t^a U_1)_{ij} (U_2 t^b)_{kl} + (U_1 t^b)_{ij} (t^a U_2)_{kl}] \left[f^{ade} f^{bd'e'} U_4^{dd'} (U_5^{ee'} - U_4^{ee'}) \right. \\ &\quad \times \left(-K - \frac{4}{z_{45}^2} + \frac{I_1}{z_{45}^2} + \frac{I_2}{z_{45}^2} \right) + 2n_f \left(\frac{I_{f1}}{z_{45}^2} + \frac{I_{f2}}{z_{45}^2} + K_f \right) \\ &\quad \left. \times \text{tr}\{t^a U_4 t^b (U_5^\dagger - U_4^\dagger)\} \right] \\ \mathcal{A}_2 &= 4(U_4 - U_1)^{dd'} (U_5 - U_2)^{ee'} \left\{ i [f^{ad'e'} (t^d U_1 t^a)_{ij} (t^e U_2)_{kl} \right. \\ &\quad - f^{ade} (t^a U_1 t^{d'})_{ij} (U_2 t^{e'})_{kl}] J_{1245} \ln \frac{z_{14}^2}{z_{15}^2} + i [f^{ad'e'} (t^d U_1)_{ij} (t^e U_2 t^a)_{kl} \\ &\quad \left. - f^{ade} (U_1 t^{d'})_{ij} (t^a U_2 t^{e'})_{kl}] J_{2154} \ln \frac{z_{24}^2}{z_{25}^2} \right\} \end{aligned} \quad (9)$$

$$\begin{aligned} \mathcal{A}_3 &= 2U_4^{dd'} \left\{ i [f^{ad'e'} (U_1 t^a)_{ij} (t^d t^e U_2)_{kl} - f^{ade} (t^a U_1)_{ij} (U_2 t^{e'} t^{d'})_{kl}] \right. \\ &\quad \times \left[\mathcal{J}_{1245} \ln \frac{z_{14}^2}{z_{15}^2} + (J_{2145} - J_{2154}) \ln \frac{z_{24}^2}{z_{25}^2} \right] (U_5 - U_2)^{ee'} \\ &\quad + i [f^{ad'e'} (t^d t^e U_1)_{ij} (U_2 t^a)_{kl} - f^{ade} (U_1 t^{e'} t^{d'})_{ij} (t^a U_2)_{kl}] \\ &\quad \left. \times \left[\mathcal{J}_{2145} \ln \frac{z_{24}^2}{z_{25}^2} + (J_{1245} - J_{1254}) \ln \frac{z_{14}^2}{z_{15}^2} \right] (U_5 - U_1)^{ee'} \right\} \end{aligned}$$

for \mathcal{A}_i kernels and

$$\begin{aligned} \mathcal{B}_1 &= 2 \ln \frac{z_{14}^2}{z_{12}^2} \ln \frac{z_{24}^2}{z_{12}^2} \left\{ (U_4 - U_1)^{ab} i [f^{bde} (t^a U_1 t^d)_{ij} (U_2 t^e)_{kl} \right. \\ &\quad + f^{ade} (t^e U_1 t^b)_{ij} (t^d U_2)_{kl}] \left[\frac{(z_{14}, z_{24})}{z_{14}^2 z_{24}^2} - \frac{1}{z_{14}^2} \right] \\ &\quad + (U_4 - U_2)^{ab} i [f^{bde} (U_1 t^e)_{ij} (t^a U_2 t^d)_{kl} \\ &\quad \left. + f^{ade} (t^d U_1)_{ij} (t^e U_2 t^b)_{kl}] \left[\frac{(z_{14}, z_{24})}{z_{14}^2 z_{24}^2} - \frac{1}{z_{24}^2} \right] \right\} \end{aligned} \quad (10)$$

$$\begin{aligned} \mathcal{B}_2 &= [2U_4^{ab} - U_1^{ab} - U_2^{ab}] [(t^a U_1)_{ij} (U_2 t^b)_{kl} \\ &\quad + (U_1 t^b)_{ij} (t^a U_2)_{kl}] \left\{ \frac{(z_{14}, z_{24})}{z_{14}^2 z_{24}^2} \left[\left(\frac{11}{3} - \frac{2n_f}{3N_c} \right) \ln \frac{z_{12}^2 \mu^2}{4} + 2C + \frac{67}{9} - \frac{\pi^2}{3} \right. \right. \\ &\quad \left. \left. - \frac{10n_f}{9N_c} \right] + \left(\frac{11}{3} - \frac{2n_f}{3N_c} \right) \left(\frac{1}{2z_{14}^2} \ln \frac{z_{24}^2}{z_{12}^2} + \frac{1}{2z_{24}^2} \ln \frac{z_{14}^2}{z_{12}^2} \right) \right\} \end{aligned} \quad (11)$$

for \mathcal{B}_i kernels. Here we used the following notations

$$\begin{aligned}
 J_{1245} &\equiv J(z_1, z_2, z_4, z_5) = \frac{(z_{14}, z_{25})}{z_{14}^2 z_{25}^2 z_{45}^2} - 2 \frac{(z_{15}, z_{45})(z_{15}, z_{25})}{z_{14}^2 z_{15}^2 z_{25}^2 z_{45}^2}, \\
 \mathcal{J}_{1245} &\equiv \mathcal{J}(z_1, z_2, z_4, z_5) \\
 &= \frac{(z_{24}, z_{25})}{z_{24}^2 z_{25}^2 z_{45}^2} - \frac{2(z_{24}, z_{45})(z_{15}, z_{25})}{z_{24}^2 z_{25}^2 z_{15}^2 z_{45}^2} \\
 &\quad + \frac{2(z_{25}, z_{45})(z_{14}, z_{24})}{z_{14}^2 z_{24}^2 z_{25}^2 z_{45}^2} - 2 \frac{(z_{14}, z_{24})(z_{15}, z_{25})}{z_{14}^2 z_{15}^2 z_{24}^2 z_{25}^2}, \\
 K &= \frac{1}{z_{45}^4} \left[\frac{z_{14}^2 z_{25}^2 + z_{15}^2 z_{24}^2 - 4z_{12}^2 z_{45}^2}{z_{14}^2 z_{25}^2 - z_{15}^2 z_{24}^2} \ln \frac{z_{14}^2 z_{25}^2}{z_{15}^2 z_{24}^2} - 2 \right] \\
 &\quad + \frac{1}{2} \left(\frac{z_{12}^4}{z_{14}^2 z_{25}^2 - z_{15}^2 z_{24}^2} \left[\frac{1}{z_{14}^2 z_{25}^2} + \frac{1}{z_{24}^2 z_{15}^2} \right] \right. \\
 &\quad \left. + \frac{z_{12}^2}{z_{45}^2} \left[\frac{1}{z_{14}^2 z_{25}^2} - \frac{1}{z_{15}^2 z_{24}^2} \right] \right) \ln \frac{z_{14}^2 z_{25}^2}{z_{15}^2 z_{24}^2}
 \end{aligned}$$

and

$$K_f = \frac{1}{z_{45}^4} \left[-2 + \frac{z_{14}^2 z_{25}^2 + z_{15}^2 z_{24}^2 - z_{12}^2 z_{45}^2}{z_{14}^2 z_{25}^2 - z_{15}^2 z_{24}^2} \ln \frac{z_{14}^2 z_{25}^2}{z_{15}^2 z_{24}^2} \right]. \tag{12}$$

The conformally invariant kernels K and K_f are parts of the NLO BK equation for dipole evolution.

Again, the result in this form is correct both in fundamental and adjoint representations so the evolution of $U \otimes U^\dagger$ and $U^\dagger \otimes U^\dagger$ can be obtained by transposition of Eqs. (9–11). If one transposes Wilson line proportional to U_2 in the l.h.s and r.h.s. of Eq. (8), takes trace of Wilson lines and adds self-interaction terms for U and U^\dagger , one reproduces after some algebra the NLO BK equation from Ref. [6]. (In doing so one can use the integral (15) below with replacements $z_3 \rightarrow z_1, z_1 \rightarrow z_2$ so that $\mathcal{J}_{22145} = \mathcal{J}_{1245}$ and $z_2 \rightarrow z_1, z_3 \rightarrow z_2$ which gives $\mathcal{J}_{12145} = J_{1245}$.) It should be noted that, although we calculated all diagrams anew, the results for two Wilson lines with open indices can be restored from the contributions of the individual diagrams in Ref. [6] since color structure of these diagrams is obvious even with open indices.

4.3. Triple interaction

The diagrams for triple interaction are shown in Fig. 2 e,f (plus permutations). The result is

$$\begin{aligned}
 &\frac{d}{d\eta} (U_1)_{ij} (U_2)_{kl} (U_3)_{mn} \\
 &= i \frac{\alpha_s^2}{2\pi^4} \int d^2 z_4 d^2 z_5 \left\{ \mathcal{J}_{12345} \ln \frac{z_{34}^2}{z_{35}^2} f^{cde} [(t^a U_1)_{ij} (t^b U_2)_{kl} \right.
 \end{aligned}$$

$$\begin{aligned}
 & \times (U_3 t^c)_{mn} (U_4 - U_1)^{ad} (U_5 - U_2)^{be} \\
 & - (U_1 t^a)_{ij} (U_2 t^b)_{kl} (t^c U_3)_{mn} (U_4 - U_1)^{da} (U_5 - U_2)^{eb} \\
 & + \mathcal{J}_{32145} \ln \frac{z_{14}^2}{z_{15}^2} f^{ade} [(U_1 t^a)_{ij} (t^b U_2)_{kl} (t^c U_3)_{mn} \\
 & \times (U_4 - U_3)^{cd} (U_5 - U_2)^{be} \\
 & - (t^a U_1)_{ij} \otimes (U_2 t^b)_{kl} (U_3 t^c)_{mn} (U_4^{dc} - U_3^{dc}) (U_5^{eb} - U_2^{eb}) \\
 & + \mathcal{J}_{13245} \ln \frac{z_{24}^2}{z_{25}^2} f^{bde} [(t^a U_1)_{ij} (U_2 t^b)_{kl} (t^c U_3)_{mn} \\
 & \times (U_4 - U_1)^{ad} (U_5 - U_3)^{ce} \\
 & - (U_1 t^a)_{ij} (t^b U_2)_{kl} (U_3 t^c)_{mn} (U_4 - U_1)^{da} (U_5 - U_3)^{ec} \Big] \Big\}, \quad (13)
 \end{aligned}$$

where

$$\begin{aligned}
 \mathcal{J}_{12345} \equiv \mathcal{J}(z_1, z_2, z_3, z_4, z_5) = & -\frac{2(z_{14}, z_{34})(z_{25}, z_{35})}{z_{14}^2 z_{25}^2 z_{34}^2 z_{35}^2} - \frac{2(z_{14}, z_{45})(z_{25}, z_{35})}{z_{14}^2 z_{25}^2 z_{35}^2 z_{45}^2} \\
 & + \frac{2(z_{25}, z_{45})(z_{14}, z_{34})}{z_{14}^2 z_{25}^2 z_{34}^2 z_{45}^2} + \frac{(z_{14}, z_{25})}{z_{14}^2 z_{25}^2 z_{45}^2}. \quad (14)
 \end{aligned}$$

As usual, the results for the evolution of $U \otimes U \otimes U^\dagger$ etc. can be obtained by transposition of color structures in Eq. (13)

The terms with two and one intersections with the shock wave coincide with Ref. [14]. When comparing the results for the diagrams with one intersection (of Fig. 2e type) to that in Ref. [14] the following integral is useful:

$$\begin{aligned}
 \int \frac{d^2 z_5}{\pi} \mathcal{J}_{12345} \ln \frac{z_{34}^2}{z_{35}^2} = & \left\{ \frac{(z_{14}, z_{24})}{2z_{14}^2 z_{24}^2} \ln \frac{z_{23}^2}{z_{24}^2} \ln \frac{z_{23}^2}{z_{34}^2} - z_2 \leftrightarrow z_3 \right\} \\
 & + \left\{ \left[\frac{(z_{14}, z_{24})(z_{24}, z_{34})}{z_{14}^2 z_{24}^2} - \frac{(z_{14}, z_{34})}{z_{14}^2} \right] \frac{1}{i\kappa_{23}} \right. \\
 & \times \left[\text{Li}_2 \left(\frac{(z_{24}, z_{34}) + i\kappa_{23}}{z_{24}^2} \right) - \text{Li}_2 \left(\frac{(z_{24}, z_{34}) - i\kappa_{23}}{z_{24}^2} \right) \right. \\
 & \left. \left. + \frac{1}{2} \ln \frac{z_{24}^2}{z_{34}^2} \ln \frac{(z_{23}, z_{24}) + i\kappa_{23}}{(z_{23}, z_{24}) - i\kappa_{23}} \right] + z_2 \leftrightarrow z_3 \right\} \quad (15)
 \end{aligned}$$

where $\kappa_{23} \equiv \sqrt{z_{24}^2 z_{34}^2 - (z_{24}, z_{34})^2}$ and Li_2 is the dilogarithm (which cancels in the final result (13)).

Note that we calculated the evolution of Wilson lines in the light-like gauge $p_2^\mu A_\mu = 0$. To assemble the evolution of colorless operators one needs to combine

these equations and connect Wilson lines by segments at infinity. These gauge links at infinity do not contribute to the kernel both in $p_2^\mu A_\mu = 0$ and Feynman gauge (note, however, that their contribution is the only non-vanishing one in $p_1^\mu A_\mu = 0$ gauge). Indeed, in the leading order it is easy to see because gluons coming from gauge links have a restriction $\alpha < e^\eta$ so the gluon connecting points x, y with $x_+ = L \rightarrow \infty$ and $z_+ = 0$ (inside the shockwave) will contain the factor $\exp(i \frac{p_1^2}{\alpha s} L)$ which vanishes for $L \rightarrow \infty$ and α restricted from above. Similarly one can prove that gauge links at infinity do not contribute to the NLO kernel and therefore the description of the evolution in terms of separate Wilson lines in the $p_2^\mu A_\mu = 0$ gauge does make sense.

5. Conclusion

We have calculated the full hierarchy of evolution equations for Wilson-line operators in the next-to-leading approximation. Two remarks, however, are in order.

First, our “building blocks” for evolution of Wilson lines are calculated at $d = 4$ ($d_\perp = 2$) so they contain infrared divergencies at large z_4 and/or z_5 , even at the leading order. For the gauge-invariant operators like color tripole or color quadrupole one can use our $d_\perp = 2$ formulas since all these IR divergencies should cancel. If, however, one is interested in the evolution of color combinations of Wilson lines (like for octet NLO BFKL¹⁵) some of the above kernels should be recalculated in $d = 4 + \epsilon$ dimensions.

Second, the NLO evolution equations presented here are “raw” evolution equations for Wilson lines with rigid cutoff (1). For example, in $\mathcal{N} = 4$ they lead to evolution equations for color dipole which is non-conformal. The reason (discussed in Ref. [7]) is that the cutoff (1) violates conformal invariance so we need an $O(\alpha_s)$ counterterm to restore our lost symmetry. For the color dipole such counterterm was found in Ref. [7] and the obtained evolution for “composite conformal dipole” is Möbius invariant and agrees with NLO BFKL kernel for two-reggeon Green function found in Ref. [16]. Thus, if one wants to use our NLO hierarchy for colorless objects such as quadrupole in $\mathcal{N} = 4$ SYM one should correct our rigid-cutoff quadrupole with counterterms which should make the evolution equation for “composite conformal quadrupole” Möbius invariant. We hope to return to the quadrupole evolution in future publications. Another example is the evolution of the three quark Wilson lines $\epsilon_{mnl}\epsilon_{m'n'l'}U_1^{mm'}U_2^{mm'}U_3^{mm'}$ (there are both pomeron and odderon contributions to this operator). After subtracting the Ref. [7] counterterms the NLO evolution equation for this operator¹⁷ becomes semi-invariant just as NLO BK in QCD. We present the NLO result for this “color tripole” in the Appendix.

Acknowledgments

This work was supported by contract DE-AC05-06OR23177 under which the Jefferson Science Associates, LLC operate the Thomas Jefferson National Accelerator Facility and by U.S. Department of Energy under Grant No. DE-SC0004286.

Appendix: rapidity evolution of “color tripole”

As an example of application of NLO hierarchy let me present the result for the evolution of three-Wilson-line operator. Similarly to the case of high-energy scattering of a meson from some hadronic target described by the interaction of that target with a color dipole corresponding to fast quark-antiquark pair, the energy dependence of scattering of a baryon can be described in terms of evolution of a three-Wilson-lines operator

$$B(z_{1\perp}, z_{2\perp}, z_{3\perp}) = U_1 \cdot U_2 \cdot U_3 \equiv \varepsilon^{i'j'h'} \varepsilon_{ijh} U_{z_1, i'}^i U_{z_2, j'}^j U_{z_3, h'}^h, \quad (16)$$

where $U_i \equiv U(z_{i\perp}, \eta)$ as usual. Similarly to the case of composite quasi-conformal dipole discussed in Ref. [7] it is convenient to consider quasi-conformal “composite tripole operator”

$$B_{123}^{\text{conf}} = B_{123} + \frac{\alpha_s}{8\pi^2} \int d\vec{r}_4 \left[\frac{\vec{r}_{12}^2}{\vec{r}_{41}^2 \vec{r}_{42}^2} \ln \left(\frac{a\vec{r}_{12}^2}{\vec{r}_{41}^2 \vec{r}_{42}^2} \right) \right. \\ \left. \times ((U_2 U_4^\dagger U_1 + U_1 U_4^\dagger U_2) \cdot U_4 \cdot U_3 - 2B_{123}) + (1 \leftrightarrow 3) + (2 \leftrightarrow 3) \right], \quad (17)$$

where we use shorthand notation $B_{mnl} \equiv B(z_{m\perp}, z_{n\perp}, z_{l\perp})$. The evolution of this composite operator has the form

$$\frac{\partial B_{123}^{\text{conf}}}{\partial \eta} = \frac{\alpha_s(\mu^2)}{8\pi^2} \int dz_4 \left\{ (B_{144} B_{324} + B_{244} B_{314} - B_{344} B_{214} - 6B_{123})^{\text{conf}} \right. \\ \times \left(\frac{z_{12}^2}{z_{41}^2 z_{42}^2} + \frac{\alpha_s}{4\pi} \left[(11 - \frac{2}{3}n_f) \left\{ \left(\frac{1}{z_{14}^2} - \frac{1}{z_{24}^2} \right) \ln \frac{z_{41}^2}{z_{42}^2} + \frac{z_{12}^2}{z_{41}^2 z_{42}^2} \ln \frac{z_{12}^2}{\mu^2} \right\} \right. \right. \\ \left. \left. + \frac{67}{3} - \pi^2 - \frac{10}{9}n_f \right] \right) + (1 \leftrightarrow 3) + (2 \leftrightarrow 3) \left\} \right. \\ - \frac{\alpha_s^2}{32\pi^3} \int dz_4 \left\{ B_{443} B_{412} \left[\frac{z_{32}^2}{z_{43}^2 z_{42}^2} \ln^2 \left(\frac{z_{32}^2 z_{14}^2}{\vec{r}_{13}^2 z_{24}^2} \right) - \frac{z_{12}^2}{\vec{r}_{41}^2 z_{42}^2} \ln^2 \left(\frac{z_{12}^2 z_{34}^2}{z_{13}^2 z_{24}^2} \right) \right] \right. \\ \left. + (\text{all 5 permutations } 1 \leftrightarrow 2 \leftrightarrow 3) \right\} \\ - \frac{\alpha_s^2 n_f}{16\pi^5} \int dz_4 dz_5 \left\{ \left(\left[\frac{1}{3} (U_1 U_4^\dagger U_5 + U_5 U_4^\dagger U_1) \cdot U_2 \cdot U_3 - \frac{1}{9} B_{123} \text{tr}(U_4^\dagger U_5) \right. \right. \right. \\ \left. \left. + (U_1 U_4^\dagger U_2) \cdot U_3 \cdot U_5 + \frac{1}{6} B_{123} - \frac{1}{5} (B_{413} B_{442} + B_{441} B_{423} - B_{412} B_{443}) \right. \right. \\ \left. \left. + (1 \leftrightarrow 2) \right] + (4 \leftrightarrow 5) \right) L_{12}^q + (1 \leftrightarrow 3) + (2 \leftrightarrow 3) \left\} \right. \\ - \frac{\alpha_s^2}{8\pi^5} \int dz_4 dz_5 \left\{ \left(\tilde{L}_{12}^C (U_4 U_5^\dagger U_2) \cdot (U_1 U_4^\dagger U_5) \cdot U_3 \right. \right. \\ \left. \left. + L_{12}^C \left[(U_4 U_5^\dagger U_2) \cdot (U_1 U_4^\dagger U_5) \cdot U_3 + \text{tr}(U_4 U_5^\dagger) (U_1 U_4^\dagger U_2) \cdot U_3 \cdot U_5 \right. \right. \right. \\ \left. \left. \left. - \frac{3}{5} (B_{155} B_{235} + B_{255} B_{135} - B_{355} B_{125}) + \frac{1}{2} B_{123} \right] \right\}$$

$$\begin{aligned}
 &+ M_{12}^C[(U_4 U_5^\dagger U_3) \cdot (U_2 U_4^\dagger U_1) \cdot U_5 + (U_1 U_4^\dagger U_2) \cdot (U_3 U_5^\dagger U_4) \cdot U_5] \\
 &+ \left. \left(\text{all 5 permutations } 1 \leftrightarrow 2 \leftrightarrow 3 \right) + (4 \leftrightarrow 5) \right\}
 \end{aligned}$$

where μ is a renormalization point in $\overline{\text{MS}}$ scheme and

$$L_{12}^C = L_{12} + \frac{z_{12}^2}{4z_{41}^2 z_{45}^2 z_{25}^2} \ln \frac{z_{42}^2 z_{15}^2}{z_{45}^2 z_{12}^2} + \frac{z_{12}^2}{4z_{42}^2 z_{45}^2 z_{15}^2} \ln \frac{z_{41}^2 z_{25}^2}{z_{45}^2 z_{12}^2}, \quad (18)$$

$$\tilde{L}_{12}^C = \tilde{L}_{12} + \frac{z_{12}^2}{4z_{41}^2 z_{45}^2 z_{25}^2} \ln \frac{z_{42}^2 z_{15}^2}{z_{45}^2 z_{12}^2} - \frac{z_{12}^2}{4z_{42}^2 z_{45}^2 z_{15}^2} \ln \frac{z_{41}^2 z_{25}^2}{z_{45}^2 z_{12}^2}, \quad (19)$$

$$\begin{aligned}
 M_{12}^C = & \frac{z_{12}^2}{16z_{42}^2 z_{45}^2 z_{15}^2} \ln \frac{z_{41}^2 z_{42}^2 z_{35}^4}{z_{43}^4 z_{15}^2 z_{25}^2} + \frac{z_{12}^2}{16z_{41}^2 z_{45}^2 z_{25}^2} \ln \frac{z_{43}^4 z_{45}^4 z_{12}^2 z_{35}^2}{z_{41}^2 z_{42}^2 z_{15}^4 z_{35}^2} \\
 & + \frac{z_{23}^2}{16z_{42}^2 z_{45}^2 z_{35}^2} \ln \frac{z_{41}^4 z_{43}^2 z_{25}^6 z_{35}^2}{z_{42}^2 z_{45}^4 z_{15}^4 z_{23}^4} + \frac{z_{23}^2}{16z_{43}^2 z_{45}^2 z_{25}^2} \ln \frac{z_{42}^2 z_{43}^2 z_{15}^4}{z_{41}^2 z_{25}^2 z_{35}^2} \\
 & + \frac{z_{13}^2}{16z_{43}^2 z_{45}^2 z_{15}^2} \ln \frac{z_{42}^4 z_{15}^2 z_{35}^2}{z_{41}^2 z_{43}^2 z_{25}^4} + \frac{z_{13}^2}{16z_{41}^2 z_{45}^2 z_{35}^2} \ln \frac{z_{42}^4 z_{15}^2 z_{35}^2}{z_{41}^2 z_{43}^2 z_{25}^2} \\
 & + \frac{z_{43}^2 z_{12}^2}{8z_{41}^2 z_{42}^2 z_{45}^2 z_{35}^2} \ln \frac{z_{41}^2 z_{43}^2 z_{25}^4}{z_{42}^2 z_{45}^2 z_{12}^2 z_{35}^2} + \frac{z_{23}^2 z_{12}^2}{8z_{41}^2 z_{42}^2 z_{25}^2 z_{35}^2} \ln \frac{z_{42}^2 z_{12}^2 z_{35}^2}{z_{41}^2 z_{23}^2 z_{25}^2} \\
 & + \frac{z_{15}^2 z_{23}^2}{8z_{41}^2 z_{45}^2 z_{25}^2 z_{35}^2} \ln \frac{z_{41}^2 z_{45}^2 z_{23}^2 z_{25}^2}{z_{42}^2 z_{15}^2 z_{35}^2}, \quad (20)
 \end{aligned}$$

$$L_{12}^q = \frac{1}{z_{04}^4} \left[\frac{z_{02}^2 z_{14}^2 + z_{01}^2 z_{24}^2 - z_{04}^2 z_{12}^2}{2(z_{02}^2 z_{14}^2 - z_{01}^2 z_{24}^2)} \ln \left(\frac{z_{02}^2 z_{14}^2}{z_{01}^2 z_{24}^2} \right) - 1 \right]. \quad (21)$$

Similarly to the case of composite dipole, the evolution of this “composite tripole” operator is a sum of the conformal part and running-coupling part explicitly proportional to β -function of QCD.

References

1. I. Balitsky, *Nucl. Phys.* **B463**, 99 (1996); “Operator expansion for diffractive high-energy scattering”, hep-ph/9706411 (1997).
2. I. Balitsky, *Phys. Rev.* **D60**, 014020 (1999).
3. I. Balitsky, “High-Energy QCD and Wilson Lines”, hep-ph/0101042 (2001).
4. I. Balitsky, “High-Energy Amplitudes in the Next-to-Leading Order”, arXiv:1004.0057 [hep-ph] (2010).
5. Yu.V. Kovchegov, *Phys. Rev.* **D60**, 034008 (1999); *Phys. Rev.* **D61**,074018 (2000).
6. I. Balitsky and G.A. Chirilli, *Phys.Rev.* **D77**, 014019(2008).
7. I. Balitsky and G.A. Chirilli, *Nucl. Phys.* **B822**, 45 (2009).
8. I. Balitsky, *Phys.Rev.* **D75**, 014001 (2007).
9. Yu. V. Kovchegov and H. Weigert, *Nucl. Phys.* **A784**, 188 (2007); *Nucl.Phys.* **A789**, 260(2007).

10. A. Kovner and M. Lublinsky, *JHEP* **0611**, 083 (2006); A. Kovner and M. Lublinsky and a Weigert, *Phys.Rev.* **D74**, 114023 (2006); F. Dominguez, C. Marquet, A. Stasto, and Bo-Wen Xiao, *Phys.Rev.* **D87** 3, 034007 (2013), E. Iancu and D.N. Triantafyllopoulos, *JHEP* **1311**, 067 (2013).
11. I. Balitsky and G.A. Chirilli, *Phys.Rev.* **D83**, 031502 (2011), *Phys.Rev.* **D87**, 014013 (2013).
12. J. Jalilian Marian, A. Kovner, A.Leonidov and H. Weigert, *Nucl. Phys.* **B504**, 415 (1997), *Phys. Rev.* **D59**, 014014 (1999); J. Jalilian Marian, A. Kovner and H. Weigert, *Phys. Rev.* **D59**, 014015 (1999); A. Kovner and J.G. Milhano, *Phys. Rev.* **D61**, 014012 (2000); A. Kovner, J.G. Milhano and H. Weigert, *Phys. Rev.* **D62**, 114005 (2000); H. Weigert, *Nucl. Phys.* **A703**, 823 (2002); E.Iancu, A. Leonidov and L. McLerran, *Nucl. Phys.* **A692**, 583 (2001), *Phys. Lett.* **B510**, 133 (2001); E. Ferreiro, E. Iancu, A. Leonidov, L. McLerran, *Nucl. Phys.* **A703**, 489 (2002).
13. A. Kovner, M. Lublinsky and Y. Mulian, *Complete JIMWLK Evolution at NLO*, e-print arXiv:1310.0378 (2013).
14. A.V. Grabovsky, *JHEP* **1309**, 141 (2013).
15. V.S. Fadin and L.N. Lipatov, *Phys.Lett.* **B706**, 470 (2012).
16. V.S. Fadin, R. Fiore and A.V. Grabovsky, *Nucl.Phys.* **B831**, 248 (2010).
17. I. Balitsky and A.V. Grabovsky, “*NLO evolution of 3-quark Wilson loop operator*”, e-print arXiv:1405.0443 (2014).